UDC 621.314 https://doi.org/10.20998/2074-272X.2024.2.09

M. Kaddache, S. Drid, A. Khemis, D. Rahem, L. Chrifi-Alaoui

Maximum power point tracking improvement using type-2 fuzzy controller for wind system based on the double fed induction generator

Introduction. *In this paper, to maximize energy transmission in wind power system, various Maximum Power Point Tracking (MPPT) approaches are available. Among these techniques, we have proposed the one based on typical fuzzy logic. Despite the somewhat reduced performance of fuzzy MPPT. For a number of reasons, fuzzy MPPT can replace conventional optimization techniques. In practice, the effectiveness of conventional MPPT methods depends mainly on the accuracy of the information given and the wind speed or knowledge of the aerodynamic properties of the wind system.* ***Novelty.*** *Our new MPPT for monitoring the maximum power point has been proposed. We developed an algorithm to improve control performance and govern the stator's developed active and reactive power using the typical fuzzy logic 2 and enable robust control of a grid-connected, doubly fed induction generator.* ***Purpose.*** *MPPT which implies the wind turbine's rotating speed should be modified in real time to capture the most wind energy, is necessary to achieve high efficiency for wind energy conversion, according to the aerodynamic characteristics of the wind turbine.* ***Methods.*** *Developing a mathematical model for a wind energy production system is complex, can be strongly affected by wind variation and is a non-linear problem. Thanks to these characteristics, thus, the Lyapunov technique is combined with a sliding mode control to ensure overall asymptotic stability and robustness with regard to parametric fluctuations in order to accomplish this goal. We contrasted our fuzzy type-2 algorithm's performance with that of the fuzzy type-1 and Perturbation & Observation (P&O) suggested in the literature.* ***Practical value****. The simulation results demonstrate that the control performance is satisfactory when using the fuzzy logic technique. From these results, it can be said for the optimization of energy conversion in wind systems, the fuzzy type-2 technique may offer a workable option. Since it presents a great possibility to avoid problems either technical or economics linked to conventional strategies.* References 21, figures 15.

Key words: **wind turbine, doubly fed induction machine, Lyapunov function, maximum power point tracking, fuzzy logic type-2, fuzzy logic type-1.**

Вступ*. У цій статті для максимізації передачі енергії у вітроенергетичній системі наведені різні підходи відстеження точки максимальної потужності (MPPT). Серед цих методів ми запропонували той, що базується на типовій нечіткій логіці. Незважаючи на дещо знижену продуктивність нечіткого MPPT. З ряду причин нечіткий MPPT може замінити звичайні методи оптимізації. На практиці ефективність звичайних методів MPPT залежить головним чином від точності наданої інформації та швидкості вітру або знання аеродинамічних властивостей вітрової системи.* ***Новизна****. Було запропоновано наш новий MPPT для моніторингу точки максимальної потужності. Ми розробили алгоритм для покращення продуктивності керування та керування розвиненою активною та реактивною потужністю статора за допомогою типової нечіткої логіки 2 та забезпечення надійного керування підключеним до мережі індукційним генератором із подвійним живленням.* ***Мета****. MPPT, який означає, що швидкість обертання вітряної турбіни має бути змінена в режимі реального часу, щоб отримувати найбільшу кількість енергії вітру, необхідна для досягнення високої ефективності перетворення енергії вітру відповідно до аеродинамічних характеристик вітрової турбіни.* ***Методи****. Розробка математичної моделі для системи виробництва вітрової енергії є складною, на неї можуть сильно впливати коливання вітру, яка є нелінійною задачею. Завдяки цим характеристикам, таким чином, метод Ляпунова поєднується з керуванням ковзним режимом для забезпечення загальної асимптотичної стабільності та стійкості щодо параметричних флуктуацій для досягнення цієї мети. Ми порівняли продуктивність нашого алгоритму нечіткого типу 2 з показниками алгоритмів нечіткого типу 1 і збурення та спостереження (P&O), запропонованих у літературі.* ***Практична цінність****. Результати моделювання демонструють, що ефективність керування є задовільною при використанні методу нечіткої логіки. З цих результатів можна сказати, що для оптимізації перетворення енергії у вітряних системах метод нечіткого типу 2 може запропонувати працездатний варіант, оскільки це чудова можливість уникнути технічних або економічних проблем, пов'язаних зі звичайними стратегіями.* Бібл. 21, рис. 15.

Ключові слова: **вітряна турбіна, асинхронна машина з подвійним живленням, функція Ляпунова, відстеження точки максимальної потужності, нечітка логіка типу 2, нечітка логіка типу 1.**

Introduction. Despite the use of windmills since antiquity, wind energy has long been forgotten. It was only after the oil crisis of 1973 that alerted the energy producing states fossil that it has known for more than 40 years an exceptional development. Indeed, from the year 2000 and in the same context of the fossil fuel market disruption, the increase electricity demand in the world and the awareness of environmental issues, these are reasons that have accentuated the need to exploit the clean energies where wind power takes a privileged place [1]. The rapid development of this technology has given rise to increasingly powerful wind turbines, whose operation increases energy efficiency, reduces mechanical efforts and improves the quality of the electrical energy produced [2]. Algeria having good wind potential, whose wind regime is moderate between 2 and 6 m/s (for 10 m from the ground) according to the wind map established by the Center for the Development of Renewable Energies (CDER) [3, 4] (Fig. 1).

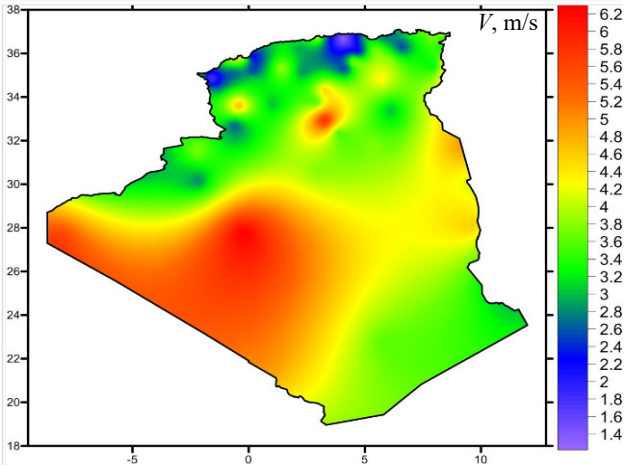

Fig. 1. Wind potential map of Algeria for 10 m from the ground, CDER [3]

The In-Salah site has an average wind speed of 6.4 m/s next to Adrar which 6.3 m/s. The Hassi-R'Mel site has fairly high average speeds reaching 6.5 m/s, whereas the province of Illizi shows speeds above 5 m/s at roughly 10 locations. As for the north of the country from west to east, various microclimates are also found. In the case of the Hauts-Plateaux, we observe that the regions of Mecheria and Tiaret have a particularly interesting average speed of 5.6 m/s. While 5.1 m/s and 5.3 m/s are recorded respectively in Djelfa and M'sila. Algeria plans to reach nearly 40 % of national electricity production from renewable sources by 2030. In addition to the installation of several photovoltaic plants in the Hauts Plateaux and the south, large wind farm projects should be built before 2024. In fact, in 2014 Algeria took delivery of the pilot Kabertène wind farm in Adrar (10 MW) and studies have been carried out to detect favorable locations in order to carry out other projects over the period 2017-2030 for a power of approximately 22 GW. Currently, variable speed wind systems based on the Doubly Fed Induction Generator (DFIG) are increasingly used on wind farms. The main advantage is the use of low power rated converters to control the slip power which is a small part of the machine rated power. By the way, the grid-connected DFIG ensures that the converters will be less in size since it permits operation across a speed range of ±30 % or less around the synchronization speed [1, 2, 5, 6]. In fact, it is a considerable economic benefit over alternative approaches (for example, the permanent magnet synchronous generator). The studied system is shown in Fig. 2. The C_p coefficient can be considered as part of the available wind power. It depends on the type and dimensions of the turbine. Generally, it is a function of the tip speed ratio λ (Fig. 3). In order to optimise the wind system, it is important to maximize C_p. To do that, we should keep the tip speed ratio at its optimal value with controlling the speed. In recent years, many researchers have focused on improving control strategy of Maximum Power Point Tracking (MPPT) based on fuzzy algorithm [7, 8].

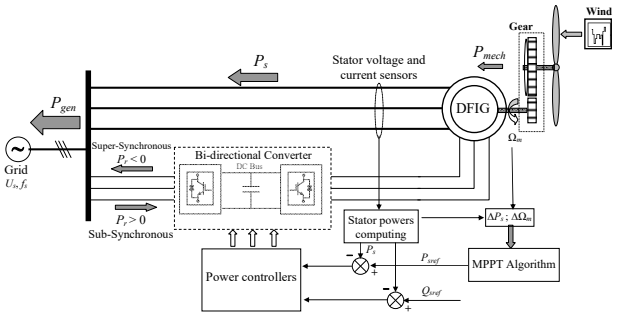

Fig. 2. Control system of the DFIG

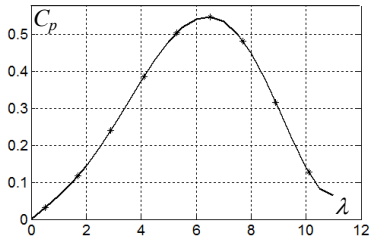

Fig. 3. Function $C_p = f(\lambda)$

The goal of the paper. In this paper, we propose a type-2 fuzzy MPPT controller. This controller will be compared with others MPPT's previously developed to demonstrate the efficiency of the proposed technique.

Modeling of wind. Turbines considering a tool for wind energy recovery on a surface S and assuming that the wind speed is identical at every point on this surface, the volume of air passing through this surface is equal to ρ, S. Consequently, the wind's incident power is kinetic and depends on the surface area that the wind sensor offers to the wind. This power P_w is defined as [9]:

$$P_w = 0.5 \cdot C_p \cdot S \cdot \rho \cdot V^3, \tag{1}$$

where P_w is the wind power; C_p is the power coefficient; S is the blades surface; ρ is the air density; V is the wind speed.

The relationship between the gear ratio is the product of the blades' linear speed and the wind speed:

$$\lambda = \Omega_t \cdot R / V, \tag{2}$$

where λ is the tip speed ratio; Ω_t is the mechanical angular speed of the wind turbine; R is the wind turbine radius.

Replacing (2) in (1), we have

$$P_w = 0.5 \cdot C_p(\lambda) \cdot S \cdot \rho \cdot \left(\frac{R}{\lambda}\right)^3 \cdot \Omega_t^3 \cdot \tag{3}$$

The following equation is used to compute the electromagnetic torque T of the turbine:

$$T = 0.5 \cdot C_p \cdot S \cdot \rho \cdot V \cdot \frac{1}{\lambda}. \tag{4}$$

The schematic diagram of the dynamic turbine model based on these equations is given in Fig. 4.

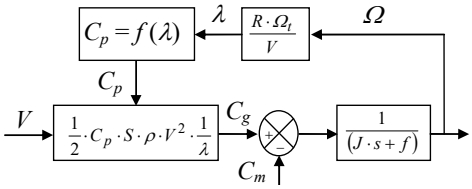

Fig. 4. Diagram of the turbine model

The DFIG model is represented by the ensuing equations in the synchronous reference frame [10]:

$$\begin{cases} \vec{V}_s = R_s \vec{I}_s + \dfrac{\mathrm{d}\vec{\phi}_s}{\mathrm{d}t} + J\omega_s \vec{\phi}_s; \\ \vec{V}_r = R_r \vec{I}_r + \dfrac{\mathrm{d}\vec{\phi}_r}{\mathrm{d}t} + J\omega_r \vec{\phi}_r, \end{cases} \tag{5}$$

where V_s, V_r, R_s, R_r, I_s, I_r, ϕ_s, ϕ_r, ω_s, ω_r are the stator and rotor voltages, resistances, currents, fluxes and current frequencies, respectively; J is the inertia moment.

The equation for current and flux is:

$$\begin{cases} \vec{I}_s = \gamma \vec{\phi}_s + \lambda \vec{\phi}_r; \\ \vec{I}_r = \lambda \vec{\phi}_s + \chi \vec{\phi}_r, \end{cases} \tag{6}$$

where

$$\gamma = 1/\sigma L_s; \quad \lambda = -M/\sigma L_s \cdot L_r; \quad \chi = 1/\sigma L_r.$$

The following equations result from equalizing the real and imaginary components of (5):

$$\begin{cases} V_{sd} = \gamma_1 \phi_{sd} - \gamma_2 \phi_{rd} + \dfrac{\mathrm{d}\phi_{sd}}{\mathrm{d}t} - \omega_s \phi_{sq} = -f_1 + \dfrac{\mathrm{d}\phi_{sd}}{\mathrm{d}t}; \\ V_{sq} = \gamma_2 \phi_{sq} - \gamma_2 \phi_{rq} + \dfrac{\mathrm{d}\phi_{sq}}{\mathrm{d}t} + \omega_s \phi_{sd} = -f_2 + \dfrac{\mathrm{d}\phi_{sq}}{\mathrm{d}t}; \\ V_{rd} = \gamma_3 \phi_{sd} + \gamma_4 \phi_{rd} + \dfrac{\mathrm{d}\phi_{rd}}{\mathrm{d}t} - \omega_r \phi_{rq} = -f_3 + \dfrac{\mathrm{d}\phi_{rd}}{\mathrm{d}t}; \\ V_{rq} = \gamma_3 \phi_{sq} + \gamma_4 \phi_{rq} + \dfrac{\mathrm{d}\phi_{rq}}{\mathrm{d}t} + \omega_r \phi_{rd} = -f_4 + \dfrac{\mathrm{d}\phi_{rq}}{\mathrm{d}t}, \end{cases} \tag{7}$$

where «*s*» and «*r*» mean stator and rotor; «*d*» and «*q*» are the direct and quadratic indicators for orthogonal component parts; and:

$$\gamma_1 = 1/\sigma\cdot\tau_s;\quad \gamma_2 = M/\sigma\cdot\tau_s\cdot L_r;\quad \gamma_3 = M/\sigma\cdot\tau_r\cdot L_s;\quad \gamma_4 = 1/\sigma\cdot\tau_r,$$

where M is the mutual inductance; σ is the leakage flux total coefficient; τ_s, τ_r are the stator and rotor time constants; L_s, L_r are the stator and rotor inductances; and:

$$\begin{cases} -f_1 = \gamma_1\phi_{sd} - \gamma_2\phi_{rd} - \omega_s\phi_{sq};\\ -f_2 = \gamma_1\phi_{sq} - \gamma_2\phi_{rq} + \omega_s\phi_{sd};\\ -f_3 = \gamma_3\phi_{sd} + \gamma_4\phi_{rd} - \omega_r\phi_{rq};\\ -f_4 = \gamma_3\phi_{sq} + \gamma_4\phi_{rq} + \omega_r\phi_{rd}. \end{cases} \tag{8}$$

The rewrite of (7) gives

$$\begin{cases} \dfrac{\mathrm{d}\phi_{sd}}{\mathrm{d}t} = f_1 + V_{sd};\\ \dfrac{\mathrm{d}\phi_{sq}}{\mathrm{d}t} = f_2 + V_{sq};\\ \dfrac{\mathrm{d}\phi_{rd}}{\mathrm{d}t} = f_3 + V_{rd};\\ \dfrac{\mathrm{d}\phi_{rq}}{\mathrm{d}t} = f_4 + V_{rq}. \end{cases} \tag{9}$$

Vector control strategy of the DFIG considers the stator voltage shown as follows in the *d-q* axis [10]:

$$\begin{cases} V_{sd} = 0;\\ V_{sq} = V_s. \end{cases} \tag{10}$$

The power expressions become

$$\begin{cases} P_s = V_s\left(\lambda\phi_{rq} + \gamma\phi_{sq}\right);\\ Q_s = V_s\left(\lambda\phi_{rd} + \gamma\phi_{sd}\right), \end{cases} \tag{11}$$

where P_s, Q_s are the stator active and reactive power.

Choosing a Lyapunov function

$$V_1 = \frac{1}{2}\left(P_s - P_{sref}\right)^2 + \frac{1}{2}\left(Q_s - Q_{sref}\right)^2 > 0. \tag{12}$$

The functions derivate is

$$\dot{V}_1 = \left(P_s - P_{sref}\right)\left(\dot{P}_s - \dot{P}_{sref}\right) + \left(Q_s - Q_{sref}\right)\left(\dot{Q}_s - \dot{Q}_{sref}\right). \tag{13}$$

Substituting (9) and (12) in (13) it results in

$$\begin{aligned} \dot{V}_1 = &\left(P_s - P_{sref}\right)\left(\alpha_1 + \lambda V_s V_{rq} - \dot{P}_{sref}\right) + \\ &+ \left(Q_s - Q_{sref}\right)\left(\alpha_2 + \lambda V_s V_{rd} - \dot{Q}_{sref}\right), \end{aligned} \tag{14}$$

with

$$\begin{cases} \alpha_1 = \lambda V_s f_4 + \gamma\left(f_2 + V_s\right);\\ \alpha_2 = \lambda V_s f_3 + \gamma f_1. \end{cases} \tag{15}$$

Equation (14) can be clearly negative, if the control law described below is established

$$\begin{cases} V_{rd} = \dfrac{1}{\lambda V_s}\left(\alpha_2 + \dot{Q}_{sref} - K_2\left(Q_s - Q_{sref}\right)\right);\\ V_{rq} = \dfrac{1}{\lambda V_s}\left(\alpha_1 + \dot{P}_{sref} - K_1\left(P_s - P_{sref}\right)\right). \end{cases} \tag{16}$$

Replacing (15) in (14) can be obtained

$$\dot{V}_1 = -K_1\left(P_s - P_{sref}\right)^2 - K_2\left(Q_s - Q_{sref}\right)^2 < 0. \tag{17}$$

So (16) is stable, if K_i (i = 1, 2) were, of course, are all positive [11], in other words

$$\begin{cases} \lim\limits_{t\to\infty}\left(Q_s - Q_{sref}\right) = 0;\\ \lim\limits_{t\to\infty}\left(P_s - P_{sref}\right) = 0. \end{cases}$$

Robust control. The robust non-linear state return control law based on Lyapunov theory is designed to address the problems of model uncertainties related to the variation of machine parameters and measurement noise [12, 13]. Model uncertainties in this type of control are generally non-linear functions [14]. Generally, the functions (f_i, α_i) are written as:

$$\begin{cases} f_i = \hat{f}_i + \Delta f_i;\\ \alpha_i = \hat{\alpha}_i + \Delta\alpha_i. \end{cases} \tag{18}$$

Replacing (18) in (9), can be obtained:

$$\begin{cases} \dfrac{\mathrm{d}\phi_{sd}}{\mathrm{d}t} = \hat{f}_1 + \Delta f + V_{sd};\\ \dfrac{\mathrm{d}\phi_{sq}}{\mathrm{d}t} = \hat{f}_2 + \Delta f + V_{sq};\\ \dfrac{\mathrm{d}\phi_{rd}}{\mathrm{d}t} = \hat{f}_3 + \Delta f + V_{rd};\\ \dfrac{\mathrm{d}\phi_{rq}}{\mathrm{d}t} = \hat{f}_4 + \Delta f + V_{rq}. \end{cases} \tag{19}$$

The new law control can be selected by taking into account Δf_i as follows:

$$\begin{cases} V_{rd} = \dfrac{1}{\lambda V_s}\begin{pmatrix} -\alpha_2 + \dot{Q}_{sref} - K_2\left(Q_s - Q_{sref}\right) - \\ - K_{22}\,\mathrm{sgn}\left(Q_s - Q_{sref}\right) \end{pmatrix};\\ V_{rq} = \dfrac{1}{\lambda V_s}\begin{pmatrix} \alpha_1 + \dot{P}_{sref} - K_1\left(P_s - P_{sref}\right) - \\ - K_{22}\,\mathrm{sgn}\left(P_s - P_{sref}\right) \end{pmatrix}. \end{cases} \tag{20}$$

where $K_{ii} \ge \beta_i$, $K_{ii} \ge 0$, K_i (i = 1, 2).

Equations (19), (20) were used to build the Lyapunov function analog from (14)

$$\begin{aligned} \dot{V}_2 = &\left(P_s - P_{sref}\right)\left(\Delta\alpha_1 - K_{11}\,\mathrm{sgn}\left(P_s - P_{sref}\right)\right) + \\ &+ \left(Q_s - Q_{sref}\right)\left(\Delta\alpha_2 - K_{22}\,\mathrm{sgn}\left(Q_s - Q_{sref}\right)\right) < 0. \end{aligned} \tag{21}$$

Therefore, if chosen, the f_i with enhanced system stability, variances can be absorbed:

$$\begin{cases} K_{11} = \left|\Delta\alpha_1\right|;\\ K_{22} = \left|\Delta\alpha_2\right|. \end{cases} \tag{22}$$

Finely, we can resume:

$$\dot{V}_1 < \dot{V}_2 < 0. \tag{23}$$

For the convergent processes stability, the control law given by (20) is applied for any α_i. The design of robust controllers is illustrated in Fig. 5.

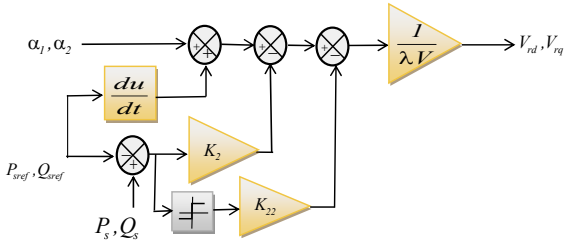

Fig. 5. Diagram design of robust controllers

New MPPT. In order to maximize the generated power, a new MPPT has been developed based on the

relationship of the aerodynamic power P, turbine speed Ω_t and electromagnetic torque T of the DFIG (Fig. 6):

$$\lambda = \Omega_t \cdot R/V\,, \tag{24}$$

$$P = 0.5 \cdot \rho \cdot R^2 \cdot V^3\,; \tag{25}$$

$$C_p = \omega \cdot T/P\,. \tag{26}$$

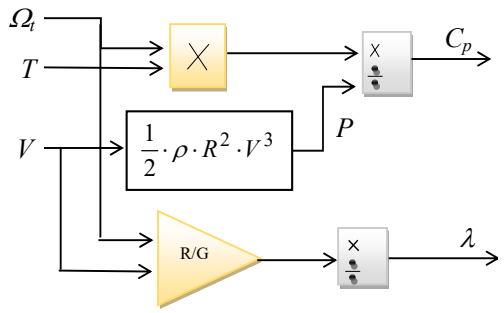

Fig. 6. New MPPT

In this research, a nonlinear empirical interpolation to represent the C_p is shown in Fig. 7.

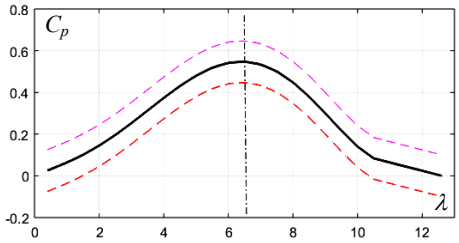

Fig. 7. Coefficient various tip speed ratio characteristic

MPPT using fuzzy logic type-2. Stator power active and speed turbine variation are the fuzzy controller's two inputs (Fig. 8).

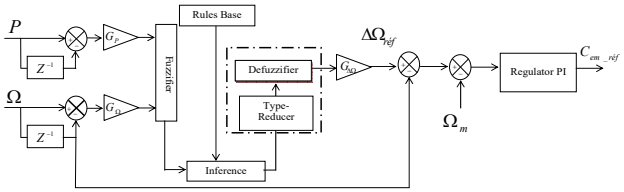

Fig. 8. Proposed fuzzy controller type-2

The definitions of error variation ΔP and $\Delta\Omega$ are [15]:

$$\begin{cases} \Delta P_s = P_s(t) - P_g(t-\Delta t) = P_g(k) - P_g(k-1); \\ \Delta\Omega_g = \Omega_m(t) - \Omega_m(t-\Delta t) = \Omega_m(k) - \Omega_m(k-1), \end{cases} \tag{27}$$

where Δt is the time step; k is the time step number.

The output of the regulator is corresponding to the coefficient variation $\Delta\dot{\Omega}_m$. The three quantities ΔP, $\Delta\Omega_m$ and $\Delta\dot{\Omega}_m$, are standardized as:

$$\begin{cases} \Delta P_g = G_p P_g\,; \\ \Delta\Omega_m = G_\Omega \Delta\Omega_m\,; \\ \Delta\dot{\Omega}_m = G_{\Delta\Omega}\Delta\dot{\Omega}_m\,, \end{cases} \tag{28}$$

where G_p, G_Ω, $G_{\Delta\Omega}$ are the scale factors or normalization, and they have a significant impact on both the control's static and dynamic performance.

The fuzzy logic type-2 membership functions for the stator active power and speed turbine variation are selected to be the same as Gaussian forms, with ΔP defined on the interval [0, 1] in Fig. 9,*a* and $\Delta\Omega_m$ is defined on the interval [–1, 1] in Fig. 9,*b*. The fuzzy logic type-2 membership functions of the variation $\Delta\dot{\Omega}_m$ are chosen with intervals formed on the interval [0, 1.2] (Fig. 9,*c*).

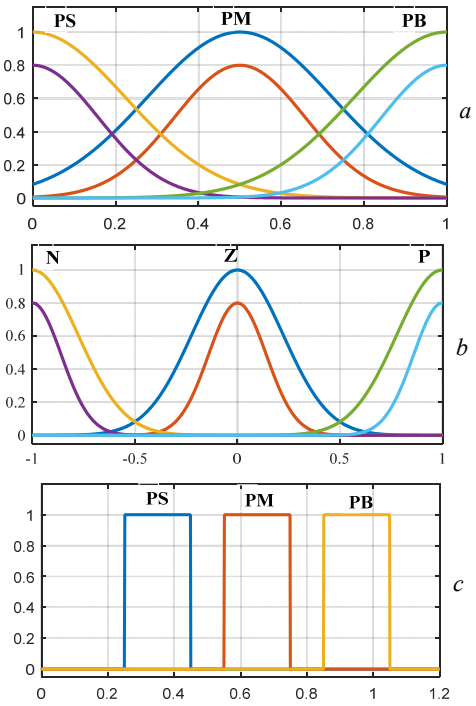

Fig. 9. Fuzzy type-2 membership functions for the variation of ΔP (*a*); $\Delta\Omega_m$ (*b*); $\Delta\dot{\Omega}_m$ (*c*)

Comparative study with fuzzy type-1 and Perturbation and Observation (P&O) algorithm. In order to show the performance of our approach based on fuzzy logic type-2, a comparison with the approach based on fuzzy logic type-1 and the P&O algorithm has been carried out [16-21].

P&O algorithm stands out because it does not need a database or training. This guarantees more versatility to this algorithm, with direct application in the system, without the need for previous information or wind speed sensors or understanding of the curve of the aerodynamic characteristics.

Figure 10 shows the P&O algorithm flow chart as it should be implemented in the control microprocessor.

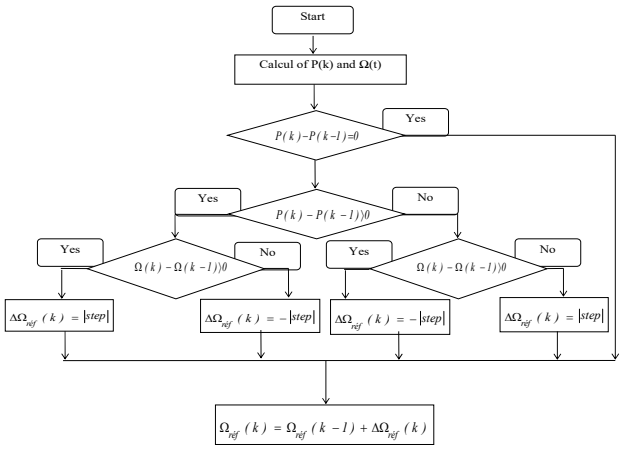

Fig. 10. P&O algorithm flow chart

Fuzzy logic type-1. For the variation of the active power of the stator ΔP and the speed of the turbine Ω_m,

their membership functions have been chosen with triangular forms and is defined on the interval [–1, 1] (Fig. 11,*a*,*b*). The membership functions type-1 of the variation of $\Delta\dot{\Omega}_m$ chosen from triangular shapes over the interval [–1, 1] (Fig. 11,*c*).

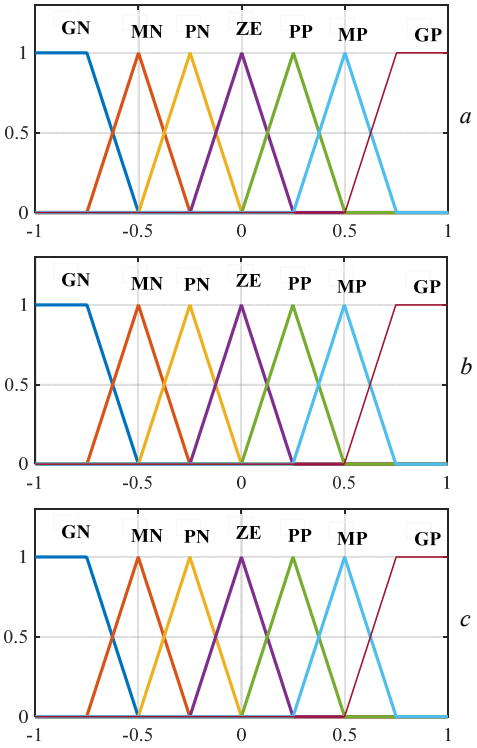

Fig. 11. Fuzzy type-1 membership functions for the variation of ΔP (*a*); $\Delta\Omega_m$ (*b*); $\Delta\dot{\Omega}_m$ (*c*)

Results. The results are arranged in accordance with the following criteria, respectively:

- simulated system with a variable wind speed with an average value of 5.8 m/s (Fig. 12);
- turbine speed (Fig. 13) fixed at 140 rad/s;
- power coefficient C_p (Fig. 14);
- stator active power (Fig. 15).

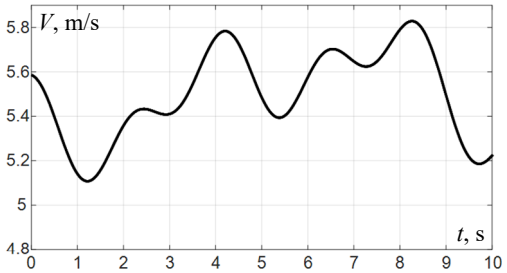

Fig. 12. Wind speed

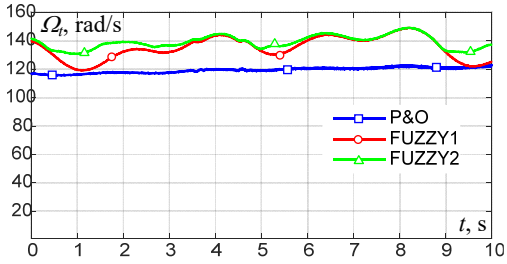

Fig. 13. Turbine speed

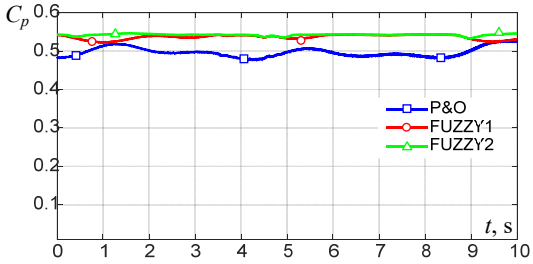

Fig. 14. Power coefficient C_p

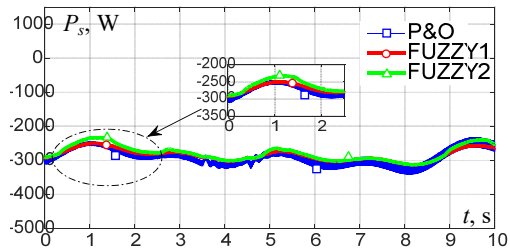

Fig. 15. Stator active power

The active power varied between –5 kW to 1 kW while the reactive power is fixed at 0 VAr. After seeing the correct follow-up of the proposed instructions it is necessary to assess the structure's robustness to parameter uncertainty. Therefore, the next step is to assess the resistance to stator and rotor change.

Finally, the results evince that the method based on fuzzy logic type-2 is superior in terms of effectiveness, robustness, and response time.

Conclusions. The results obtained show the performance of our type-2 fuzzy maximum power point tracking (MPPT) compared to two other techniques (Perturbation and Observation) and type-1 fuzzy. For several reasons, the latter technique can replace conventional optimization techniques. In practice, the effectiveness of conventional MPPT methods depends mainly on the accuracy of the information given and the wind speed or the knowledge of the aerodynamic properties of the wind system. However, this need an anemometer, which raises the systems cost. Thus, knowledge of aerodynamic properties requires the manufacturer to carry out tests that are a bit complex and expensive. In addition, these characteristics change from turbine to turbine. They also vary with climatic conditions, which decrease the reliability of the system. It is better to choose the command strategies that do not depend on these parameters.

Conflict of interest. The authors of the article declare that there is no conflict of interest.

REFERENCES

1. Belkacem Y., Drid S., Makouf A., Chrifi-Alaoui L. Multi-agent energy management and fault tolerant control of the micro-grid powered with doubly fed induction generator wind farm. *International Journal of System Assurance Engineering and Management*, 2022, vol. 13, no. 1, pp. 267-277. doi: https://doi.org/10.1007/s13198-021-01228-2.

2. Slimane W., Benchouia M.T., Golea A., Drid S. Second order sliding mode maximum power point tracking of wind turbine systems based on double fed induction generator. *International Journal of System Assurance Engineering and Management*, 2020, vol. 11, no. 3, pp. 716-727. doi: https://doi.org/10.1007/s13198-020-00987-8.

3. Guezgouz M., Jurasz J., Chouai M., Bloomfield H., Bekkouche B. Assessment of solar and wind energy

complementarity in Algeria. *Energy Conversion and Management*, 2021, vol. 238, art. no. 114170. doi: https://doi.org/10.1016/j.enconman.2021.114170.
4. Daaou Nedjari H., Haddouche S.K., Balehouane A., Guerri O. Optimal windy sites in Algeria: Potential and perspectives. *Energy*, 2018, vol. 147, pp. 1240-1255. https://doi.org/10.1016/j.energy.2017.12.046.
5. Galdi V., Piccolo A., Siano P. Exploiting maximum energy from variable speed wind power generation systems by using an adaptive Takagi–Sugeno–Kang fuzzy model. *Energy Conversion and Management*, 2009, vol. 50, no. 2, pp. 413-421. doi: https://doi.org/10.1016/j.enconman.2008.09.004.
6. Abdeddaim S., Betka A., Drid S., Becherif M. Implementation of MRAC controller of a DFIG based variable speed grid connected wind turbine. *Energy Conversion and Management*, 2014, vol. 79, pp. 281-288. doi: https://doi.org/10.1016/j.enconman.2013.12.003.
7. Hemeyine A., Abbou A., Tidjani N., Mokhlis M., Bakouri A. Robust Takagi Sugeno Fuzzy Models control for a Variable Speed Wind Turbine Based a DFI-Generator. *International Journal of Intelligent Engineering and Systems*, 2020, vol. 13, no. 3, pp. 90-100. doi: https://doi.org/10.22266/ijies2020.0630.09.
8. Hemeyine A.V., Abbou A., Bakouri A., Labbadi M., El Moustapha S.M.o.M. Power Control for Wind Turbine Driving a Doubly Fed Induction Generator using Type-2 Fuzzy Logic Controller. *2019 7th International Renewable and Sustainable Energy Conference (IRSEC)*, 2019, pp. 1-6. doi: https://doi.org/10.1109/IRSEC48032.2019.9078146.
9. Lei Y., Mullane A., Lightbody G., Yacamini R. Modeling of the Wind Turbine With a Doubly Fed Induction Generator for Grid Integration Studies. *IEEE Transactions on Energy Conversion*, 2006, vol. 21, no. 1, pp. 257-264. doi: https://doi.org/10.1109/TEC.2005.847958.
10. Cheikh R., Menacer A., Drid S. Robust control based on the Lyapunov theory of a grid-connected doubly fed induction generator. *Frontiers in Energy*, 2013, vol. 7, no. 2, pp. 191-196. doi: https://doi.org/10.1007/s11708-013-0245-y.
11. Bodson M., Chiasson J. Differential-geometric methods for control of electric motors. *International Journal of Robust and Nonlinear Control*, 1998, vol. 8, no. 11, pp. 923-954. doi: https://doi.org/10.1002/(SICI)1099-1239(199809)8:11<923::AID-RNC369>3.0.CO;2-S.
12. Mahboub M.A., Drid S., Sid M.A., Cheikh R. Robust direct power control based on the Lyapunov theory of a grid-connected brushless doubly fed induction generator. *Frontiers in Energy*, 2016, vol. 10, no. 3, pp. 298-307. doi: https://doi.org/10.1007/s11708-016-0411-0.
13. Khalil H.K. Adaptive output feedback control of nonlinear systems represented by input-output models. *IEEE Transactions on Automatic Control*, 1996, vol. 41, no. 2, pp. 177-188. doi: https://doi.org/10.1109/9.481517.
14. Drid S., Makouf A., Nait-Said M.S, Tadjine M. The doubly fed induction generator robust vector control based on Lyapunov Method. *Transactions on Systems, Signals & Devices*, 2009, vol. 4, no. 2, pp. 237-249.
15. Kaddache M., Drid S., Khemis A., Rahem D., Chrifi-Alaoui L., Drid M.D. Fuzzy-type-2 maximum power tracking controller of the double fed wind generator. *2022 IEEE 21st International Conference on Sciences and Techniques of Automatic Control and Computer Engineering (STA)*, 2022, pp. 512-515. doi: https://doi.org/10.1109/STA56120.2022.10019178.
16. Kim I.-S., Kim M.-B., Youn M.-J. New Maximum Power Point Tracker Using Sliding-Mode Observer for Estimation of Solar Array Current in the Grid-Connected Photovoltaic System. *IEEE Transactions on Industrial Electronics*, 2006, vol. 53, no. 4, pp. 1027-1035. doi: https://doi.org/10.1109/TIE.2006.878331.
17. Hessad M.A., Bouchama Z., Benaggoune S., Behih K. Cascade sliding mode maximum power point tracking controller for photovoltaic systems. *Electrical Engineering & Electromechanics*, 2023, no. 1, pp. 51-56. doi: https://doi.org/10.20998/2074-272X.2023.1.07.
18. Abid M., Laribi S., Larbi M., Allaoui T. Diagnosis and localization of fault for a neutral point clamped inverter in wind energy conversion system using artificial neural network technique. *Electrical Engineering & Electromechanics*, 2022, no. 5, pp. 55-59. doi: https://doi.org/10.20998/2074-272X.2022.5.09.
19. Akkouchi K., Rahmani L., Lebied R. New application of artificial neural network-based direct power control for permanent magnet synchronous generator. *Electrical Engineering & Electromechanics*, 2021, no. 6, pp. 18-24. doi: https://doi.org/10.20998/2074-272X.2021.6.03.
20. Khemis A., Boutabba T., Drid S. Model reference adaptive system speed estimator based on type-1 and type-2 fuzzy logic sensorless control of electrical vehicle with electrical differential. *Electrical Engineering & Electromechanics*, 2023, no. 4, pp. 19-25. doi: https://doi.org/10.20998/2074-272X.2023.4.03.
21. Sahraoui H., Mellah H., Drid S., Chrifi-Alaoui L. Adaptive maximum power point tracking using neural networks for a photovoltaic systems according grid. *Electrical Engineering & Electromechanics*, 2021, no. 5, pp. 57-66. doi: https://doi.org/10.20998/2074-272X.2021.5.08.

Received 20.07.2023
Accepted 03.10.2023
Published 02.03.2024

M. Kaddache[1], *PhD Student*,
S. Drid[2], *PhD*, *Professor*,
A. Khemis[3], *Doctor of Technical Science*, *Associate Professor*,
D. Rahem[1], *PhD*, *Professor*,
L. Chrifi-Alaoui[4], *PhD*, *Professor*,
[1] Laboratoire de Génie Electrique et Automatique (LGEA),
University of Oum El Bouaghi,
B.P 358 Route de Constantine, Oum El Bouaghi, 04000, Algeria,
e-mail: kaddache.mouna@gmail.com; rahem_djamel@yahoo.fr
[2] Higher National School of Renewable Energies, Environment and Sustainable Development,
53, Constantine Road, Fesdis, Batna, 05078, Algeria,
e-mail: s.drid@hns-re2sd.dz (Corresponding Author)
[3] University of Khenchela,
El-Hamma, BP 1252 Road of Batna, Khenchela, 40004, Algeria,
e-mail: khemis05@yahoo.fr
[4] Laboratoire des Technologies Innovantes (LTI),
University of Picardie Jules Verne, Amiens, 80000, France,
e-mail: larbi.alaoui@u-picardie.fr

How to cite this article:
Kaddache M., Drid S., Khemis A., Rahem D., Chrifi-Alaoui L. Maximum power point tracking improvement using type-2 fuzzy controller for wind system based on the double fed induction generator. *Electrical Engineering & Electromechanics*, 2024, no. 2, pp. 61-66. doi: https://doi.org/10.20998/2074-272X.2024.2.09